

# Electrosynthesis and characterization of an electroactive material from 2-(3-Thienyl) ethyl acrylate

Y. L. QIAO, L. HAN, Y. B. DING\*, L. SHEN

*The Department of Coatings and Polymeric Materials, College of Chemistry and Chemical Engineering, Jiangxi Science & Technology Normal University, Nanchang 330013, P. R. China*

The radical copolymerization of 3-ethyl acrylate-thiophene (TE-AA) and acrylic acid (AA) led to form the precursor polymer, thienyl-group-bearing acrylate polymer (TE-PAA-co-PAA), and free-standing acrylate polymer modified poly(3-thienylethanol) (PTE-PAA-co-PAA) films were synthesized electrochemically by direct anodic oxidation of TE-PAA-co-PAA. The electrochemical, optical, thermal property and morphology of obtained polymer (PTE-PAA-co-PAA) were systematically studied via cyclic voltammetry, FT-IR, UV-Vis spectra, fluorescence spectra, thermogravimetry and scanning electron microscopy (SEM). Cyclic voltammetry studies demonstrated that the precursor can be reversibly oxidized and reduced accompanied by obvious color changes from dark blue to transmissive yellow-green and the electroactive polymer has good redox activity as well as good electrochemical stability. Additionally, the fluorescence spectra showed that the so-obtained crosslinked polymer is still good blue-light emitter.

(Received July 21, 2016; accepted November 28, 2017)

**Keywords:** 3-Ethyl acrylate-thiophene, Free radical polymerization, PTE-PAA-co-PAA copolymer, Electrochemical polymerization, Crosslinked network film

## 1. Introduction

Conducting polymers (CPs) have attracted considerable attention for their promising application rechargeable battery, electrochromic display, antistatic and anticorrosive coating, electrode materials and sensor [1, 2].

Among these numerous conducting polymers, poly(thiophene) (PT) and its derivatives have rapidly become the subject of considerable interest [3]. But, the stiff polyconjugation chains seriously influence the processability of PT, which ultimately restrict their applied ranges and areas. Some changes in the structure of PT are needed to afford processability. As a matter of fact, various methods can be used to improve mechanical properties of PT [4]. Towards the goal of obtaining processable polyconjugated thiophene, recent works in the literature have dealt with graft reactions of thiophene onto processible matrices [5]. Such as methacrylate and acrylate functionalized PEDOT was obtained in Kim and Xu laboratory [6-7], and exhibited desirable electrochromic (EC) performance. Besides, 3-thiophene ethanol (TE) has been used to synthesize different thiophene-based precursor bearing various functional groups [8-9]. And these results showed that substituent of the conjugated block not only turn the oxidation potential of the precursor, but also modulate the solubility, optical property and band gap of the corresponding polymer.

Therefore, in order to obtain a polymer with both polythiophene side-chains and the processability of the precursor polymer, the acrylic polymers were introduced into thiophene ring to obtain a precursor, and the corresponding polymer (PTE-PAA-co-PAA) was electrochemically synthesized. In addition, the properties of PTE-PAA-co-PAA, including the electrochemical, optical and thermal property were systematically explored.

## 2. Experimental

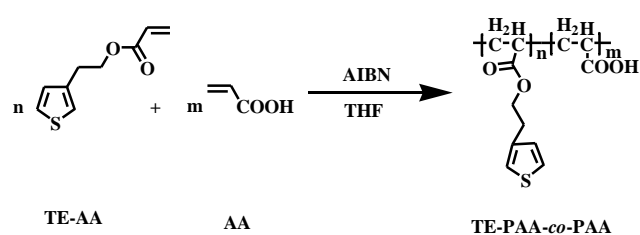
### 2.1. Chemicals and apparatus

3-ethyl acrylate-thiophene (TE-AA) was synthesized according to the method reported elsewhere [10]. Azodiisobutyronitrile (AIBN) was purchased from Aladdin Industrial Corporation and used without further purification. Boron trifluoride diethyl etherate (BFEE) was purchased from Beijing Xin'ao Xunchi Chemicals Co. Ltd., China and used after vacuum distillation. Dichloromethane (DCM) and tetrahydrofuran (THF) as well as acrylic acid (AA) were all analytical grade and purchased from Beijing Chemical Works and used after reflux distillation. Infrared spectra were recorded using a Bruker Vertex 70 Fourier transform infrared (FT-IR) spectrometer with samples in KBr pellets. But, it is so difficult to grind the resultant crosslinked polymers into

powder that their IR characterization only can be processed using attenuated total reflectance (ATR-FTIR). The UV-Vis spectra were detected with Agilent 8453 spectrometer. The fluorescence spectra were determined with an F-4500 fluorescence spectrophotometer (Hitachi). Gel permeation chromatography (GPC) (poly(methyl methacrylate) as interior label) measurements of the samples were performed in high purity solvent tetrahydrofuran with a Waters Breeze GPC system. Thermogravimetric analysis (TGA) was performed with a Pyris Diamond TG/DTA thermal analyzer (Perkin-Elmer). Scanning electron microscopy (SEM) measurements were made with a cold field emission scanning electron microscope JSM-6701F.

## 2.2. Preparation of the precursor TE-PAA-co-PAA

The precursor *TE-PAA-co-PAA* was synthesized according to literature procedures [11], as exhibited in Scheme 1.



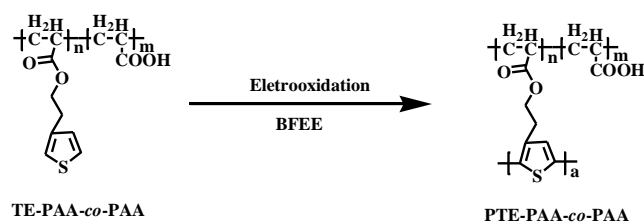
Scheme 1. Preparation of the precursor *TE-PAA-co-PAA*

A 50 mL round-bottom flask containing TE-AA (50 mmol, 9.10 g), AA (50 mmol, 3.61 g) and AIBN (0.2 mmol, 0.0328 g) in 50 mL of THF was sealed under a nitrogen atmosphere. After the reaction mixture was stirred for 2 days at 60 °C, it was concentrated to remove vast solvent. The polymer was first precipitated in methanol, and then redissolved in methylene chloride. After reprecipitation in methanol, *TE-PAA-co-PAA* was obtained as a claybank solid. The molecular weight of *TE-PAA-co-PAA* was determined by GPC in chromatographically pure tetrahydrofuran (against poly(methyl methacrylate) standards):  $M_n=11061$  g/mol,  $M_w=41851$  g/mol,  $M_w/M_n=3.78$ .

## 2.3. Electrochemical synthesis of the crosslinked network film PTE-PAA-co-PAA

Electrochemical tests and polymerization of precursor (Scheme 2) were performed in a one-compartment cell using a potentiostat-galvanostat (model 263, EG&G Princeton Applied Research) under computer control. For electrochemical tests, counter electrodes was Pt wire with diameter of 1 mm, an Ag/AgCl electrode was used as reference electrode (RE), they were placed 1cm apart

during the tests. To obtain a sufficient amount of the polymer films for characterization, ITO with surface areas of 2 and 2 cm<sup>2</sup> each was used as the working electrode. These electrodes were immersed then carefully polished with ethanol and then dried in air before each experiment. The typical electrolytic solution containing 2.26 g L<sup>-1</sup> precursors *TE-PAA-co-PAA* was used. All the solutions were deaerated by a dry nitrogen stream and maintained under a slight overpressure through all the experiments. The amount of polymer deposited on the electrode was controlled by the integrated charge passed through the cell. The polymer films were grown potentiostatically, and their thickness was controlled by the total charge passed through the cell, which was read directly from the current-time (I-t) curves by a computer. In order to remove the electrolyte and oligomer/monomer, the electropolymerized films were rinsed in mixtures of acetone and water containing increasing amounts of water and finally pure water. For spectral analyses, the polymer films were dedoped with 25% ammonia for 3 days, and then washed repeatedly with pure water. Finally, the polymer films were dried at 60 °C under vacuum for 24 h.



Scheme 2. Electrochemical synthesis of the crosslinked network film *PTE-PAA-co-PAA*

## 3. Results and discussion

### 3.1. Electrochemistry

In general, the lower oxidation potential is beneficial to obtain high-quality film without peroxidation leading to conducting polymers with poor properties and even destroying their structures for thiophene rings [12]. As seen from Fig. 1A, the onset oxidation potential of precursor polyacrylate modified thiophene *TE-PAA-co-PAA* was 1.06 V in DCM + 50% BFEE, clearly lower than 1.35 V of thiophene in acetonitrile with 80% BFEE. Fig. 1B shows the successful CVs of *TE-PAA-co-PAA* during the scanning range of -0.1 V and 1.3 V, which, the same as other precursor with electroactive groups expresses good electrochemical activity and obvious broad redox peak emerging at 0.88 V and 0.44 V, respectively. With the scanning cycle gradually increasing, the overpotential is required to overcome the increasing electrical resistance [13], resulting to a clear potential shift and the evolution of peak current density.

The CVs of PTE-PAA-co-PAA film deposited on ITO were recorded in monomer-free DCM + 50% BFEE under different potential scanning rates for comparison during the scanning range of 0–0.95 V in Fig. 1C. Similar to the results reported previously, the steady-state CVs displayed broad anodic and cathodic peaks and the peak current densities were proportional to the potential scan rates (inset), indicating that the redox processes were not controlled by diffusion limits and the electroactive polymers were well adhered to the working electrode surface [14]. Furthermore, these polymer films could be repeatedly cycled between the conducting (oxidized) and insulating (neutral) states from 0.59 to 0.27 V at the scan rate of  $150 \text{ mV s}^{-1}$  without significant decomposition, indicating the high redox stability of PTE-PAA-co-PAA. The electrochemical stability, as a performance characterization, decided that whether the so-prepared conducting polymer could be applied to electric components extensively. So, the long-time cyclic voltammetry method came into being. The electrochemical stability of resultant PTE-PAA-co-PAA film was shown in Fig. 1D. After 1000 cycles and 2000 cycles, the total electrochemical activity with 88.11% and 73.67% remained, respectively. In conclusion, so-prepared electroactive polymer was endowed with great electrochemical stability.

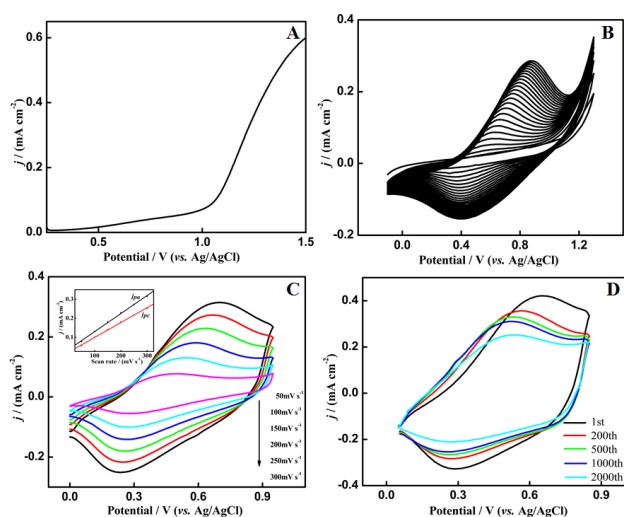


Fig. 1. Anodic polarization curve (A) and cyclic voltammogram (B) of  $2.26 \text{ g L}^{-1}$  TE-PAA-co-PAA in the electrolyte of DCM + 50% BFEE. Cyclic voltammograms under different potential scanning rates (C) and upon repeated cycling (D) of PTE-PAA-co-PAA in DCM + 50% BFEE without precursor. Inset: plots of redox peak current densities vs. potential scan rates

### 3.2. FT-IR spectra

According to the IR spectrum of TE-PAA-co-PAA (Fig. 2-b), the absorption at  $3109 \text{ cm}^{-1}$  was produced by

C-H vibration of the 2, 5-positions in the thiophene ring, but disappeared in the electrochemical polymerized sample (Fig. 2c), indicated the thiophene was very stable during the polymerization process and the electropolymerization of TE-PAA-co-PAA occurred at the 2,5-positions of the thiophene ring. The C=O vibration frequency for the ester group appeared as a large peak at  $1726 \text{ cm}^{-1}$  in both PTE-PAA-co-PAA and TE-PAA-co-PAA with no detectable change in intensity or wavelength.

The bands at  $1443 \text{ cm}^{-1}$  and  $1391 \text{ cm}^{-1}$  can be ascribed to the C=C stretching vibrations of the thiophene ring and C-C skeletal stretching [15]. Compared with that of TE-AA, the C=C stretching vibration frequency ( $1627 \text{ cm}^{-1}$ ) of TE-PAA-co-PAA disappeared after free radical polymerization, which is direct proof of the polymerization of the acrylate groups [7].”

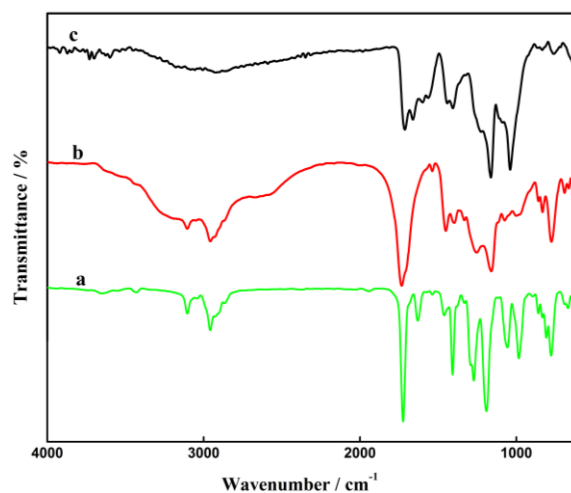


Fig. 2. FT-IR spectra of TE-AA (a), TE-PAA-co-PAA (b) and PTE-PAA-co-PAA (c)

### 3.3. Optical properties

Fig. 3A shows the UV-visible spectra of TE-PAA-co-PAA in THF (inset) as well as the doped (a) and dedoped (b) PTE-PAA-co-PAA films deposited on ITO. The spectrum of the doped film showed a characteristic absorption at about 364 nm and a much broader absorption from 492 nm to 822 nm, which were caused by the valence band-conduction band ( $\pi-\pi^*$ ) transition in the long conjugated chain and conductive species such as polaron or bipolaron, respectively [16]. On the other hand, the spectrum of the dedoped films showed a narrow maximum absorption wavelength ( $\lambda_{\text{max}}$ ) at 397 nm and a much broader absorption from 577 nm to about 964 nm, which was a red shift in contrast to doped film due to the departure of conductive species [17]. In addition, in contrast with precursor TE-PAA-co-PAA ( $\lambda_{\text{max}}=231 \text{ nm}$ ), the absorption peaks of PTE-PAA-co-PAA experienced obvious red shift, which implied that the conjugated chain

had been extended [18]. Moreover, the fluorescence properties of resultant crosslinked polymer PTE-PAA-co-PAA in the doped (Fig. 3B-a) and dedoped (Fig. 3B-b) states on a transparent ITO was investigated. From the insets of Fig. 3B, it could be indicated that the emission peaks of TE-PAA-co-PAA emerged at 340 nm, while for the polymer PTE-PAA-co-PAA, the emission peaks appeared at 482 nm for the doped state and 486 nm for the dedoped state. Compared with the emission peaks of TE-PAA-co-PAA, the emission peaks of PTE-PAA-co-PAA experienced clear red shift, which showed that the oxidation polymerization of thiophene rings had occurred [19]. And it is expected to be utilized in blue-light organic light-emitting device.

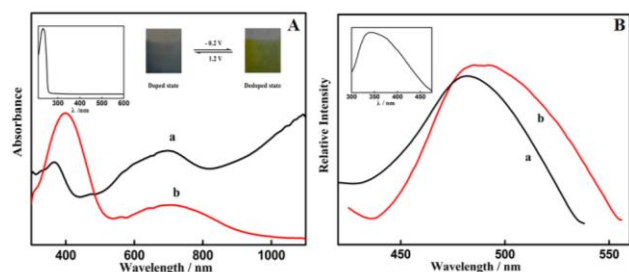


Fig. 3. UV-Vis spectra (A) and fluorescence spectra (B) of TE-PAA-co-PAA in THF (inset) and the doped (a) and dedoped (b) PTE-PAA-co-PAA film coated on an optically transparent ITO electrode

### 3.4. Thermal property and morphology

Fig. 4A presents the TGA and DTG curves of PTE-PAA-co-PAA film. During the temperature range between 360 K and 728 K, it had a prominent weight loss with 57.33%. This weight loss can be ascribed to the oxidizing decomposition of the skeletal PTE and/or PAA backbone chain structures. Moreover, it can be seen from Fig. 4B, microscopically, doped PTE-PAA-co-PAA film was tumor-like aggregation, which facilitates the movement of doping anions in and out of the polymer film during doping and dedoping process, in well accordance with the good redox activity. While the dedoped PTE-PAA-co-PAA film (inset) was defective due to the leaving of opposite anion from the surface or body of film. Macroscopically, the PTE-PAA-co-PAA film was flat, compact and smooth and can be peeled off directly in the shape of free-standing film. That is, the conducting polymer with the structures was extremely beneficial to improve their electrical conductivity and electron transfer capability and also make them good candidates for potential applications, such as ion-selective electrodes [20], ion-sieving films and matrices for hosting catalyst particles.

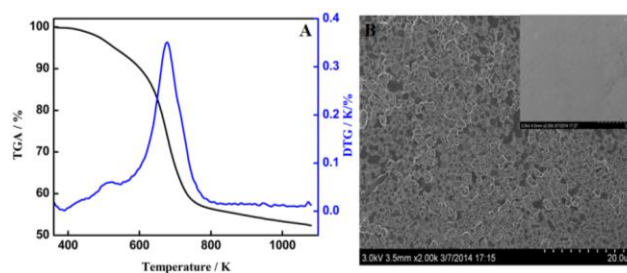


Fig. 4. TG curve (black) and DTG curve (blue) of the dedoped PTE-PAA-co-PAA film (A) and the SEM photograph of the doped PTE-PAA-co-PAA film (B). Inset: the SEM photograph of the dedoped PTE-PAA-co-PAA film

## 4. Conclusions

In conclusion, acrylate functionalized TE-PAA-co-PAA was synthesized, and its corresponding polymer PTE-PAA-co-PAA was also electrosynthesis under optimal conditions. As formed polymer film PTE-PAA-co-PAA showed good redox activity and long-term stability in monomer-free DCM + 50% BFEE, and smooth and compact morphology. Additionally, fluorescence spectra show that the so-obtained crosslinked polymer is still good blue-light emitter. These properties make PTE-PAA-co-PAA a good candidate for commercial applications.

## Acknowledgements

The National Natural Science Foundation of China (51263011) is gratefully acknowledged for support.

## References

- [1] N. Aydemir, J. Malmström, J. Travascejdic, *Physical Chemistry Chemical Physics* **18**(12), 8264 (2016).
- [2] M. Ates, *Journal of Adhesion Science and Technology* **30**(14), 1510 (2016).
- [3] B. Massoumi, A. Farnoudian-Habibi, M. Jaymand, *Journal of Solid State Electrochemistry* **20**(2), 489 (2016).
- [4] N. Ranieri, G. Ruggeri, F. Ciardelli, *Polymer International* **48**(11), 1091 (1999).
- [5] J. Kim, J. You, B. Kim, T. Park, E. Kim, *Advanced Materials* **23**(36), 4168 (2011).
- [6] J. Kim, J. You, E. Kim, *Macromolecules* **43**(5), 2322 (2010).
- [7] L. Qin, J. Xu, B. Lu, Y. Lu, X. Duan, G. Nie, *Journal of Materials Chemistry* **22**(35), 18345 (2012).
- [8] P. J. Costanzo, K. K. Stokes, *Macromolecules* **35**(18), 6804 (2002).
- [9] L. Sacan, A. Cirpan, P. Camurlu, L. Toppare, *Synthetic metals* **156**(2), 190 (2006).

- [10] M. L. Hallensleben, F. Hollwedel, D. Stanke, *Macromolecular Chemistry and Physics* **196**(11), 3535 (1995).
- [11] L. Han, Y. Qiao, W. Zhou, L. Shen, J. Xu, *Advanced Materials Research* **2014**(1053), 245 (2014).
- [12] J. Wang, H. Miao, B. Lu, J. Xu, Y. Li, H. Zhang, *Acta Polymerica Sinica* **11**(3), 327 (2011).
- [13] T. Otero, E. Larreta-Azelain, *Polymer* **29**(8), 1522 (1988).
- [14] K. Lin, S. Zhen, S. Ming, J. Xu, B. Lu, *New Journal of Chemistry* **39**(3), 2096 (2015).
- [15] D. Motaung, G. Malgas, C. Arendse, T. Malwela, *Materials Chemistry & Physics* **124**(1), 208 (2010).
- [16] G. Sönmez, I. Schwendeman, P. Schottland, K. Zong, J. Reynolds, *Macromolecules* **36**(3), 639 (2003).
- [17] D. E. Labaye, C. Jérôme, V. M. Geskin, P. Louette, R. Lazzaroni, L. Martinot, R. Jerome, *Langmuir* **18**(13), 5222 (2002).
- [18] B. Lu, J. Yan, J. Xu, S. Zhuo, X. Xu, *Macromolecules* **43**(10), 4599 (2010).
- [19] P. J. Costanzo, K. K. Stokes, *Macromolecules* **35**(18), 6804 (2002).
- [20] A. Rzewuska, M. Wojciechowski, E. Bulska, E. A. H. Hall, K. Maksymiuk, A. Michalska, *Analytical Chemistry* **80**(1), 321 (2008).

---

\*Corresponding author: 1985yongboding@tongji.edu.cn